Design of Waveguide-to-Orotron-Resonator Transition with Modified Bethe Theory

G. Faby and K. Schünemann, *Fellow, IEEE*

***Abstract*— The modified Bethe theory is applied to the waveguide-to-resonator transition, which is used for output coupling in an orotron oscillator designed for operation at 94 GHz. The finite thickness of the coupling hole between output waveguide and resonator is taken into account. The approach results in an equivalent circuit, which describes the reflection-type resonator, with respect to the output waveguide. Its equivalent circuit parameters are given in closed-form expressions. The calculated reflection coefficients are compared to experimental results. The assumed single-mode operation in the resonator is demonstrated by field-profile measurements.**

***Index Terms*—Electromagnetic coupling, optical resonator, Q measurements.**

I. Introduction

OPEN resonators have been studied intensively in the past [1], [2]. In the millimeter-wave range, the most important application has been in the determination of electrical properties of dielectric materials [3], [4] due to the high quality (Q) factor of a quasi-optical resonator. For these applications, the change of the unloaded Q factor due to the characteristics of the probe has to be measured. Since for this task the resonator is only weakly coupled to the waveguide, there has been little work on the tight coupling of open resonators. However, in the last years, strongly coupled open resonators have gained more interest due to their application in high-power tubes [5], [6].

This paper deals with an orotron resonator. The orotron has been proposed [7] and developed [8] some time ago as a promising (sub)millimeter-wave source with moderate-to-medium output power levels.

The design of the cold cavity used in the orotron is very important for optimum oscillator performance. Especially the loaded Q factor can be utilized to achieve optimum efficiency. Fig. 1 demonstrates this behavior, which has been presented in [9]. Since the unloaded Q factor is fixed for a desired working mode, the loaded Q factor can be adjusted varying the parameters of the coupling hole. Although there are some investigations on electrical tuning of the coupling during operation by means of a semitransparent lower mirror [10], the simplest way is to design the coupling hole knowing the dependence of the resonator coupling on the geometric parameters of the aperture.

Manuscript received April 2, 1997; revised July 18, 1997. This work was supported by the Deutsche Forschungsgemeinschaft.

The authors are with the Technische Universität Hamburg–Harburg, Arbeitsbereich Hochfrequenztechnik, D-21071 Hamburg, Germany.

Publisher Item Identifier S 0018-9480(97)08022-8.

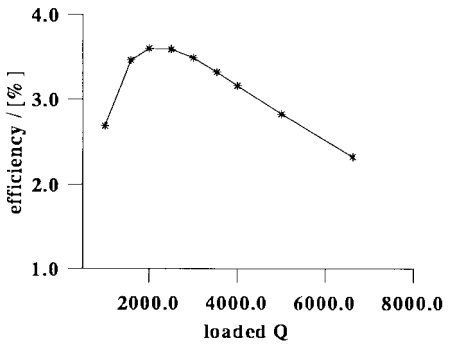

Fig. 1. Simulated efficiency of a 94-GHz orotron versus loaded Q factor [9].

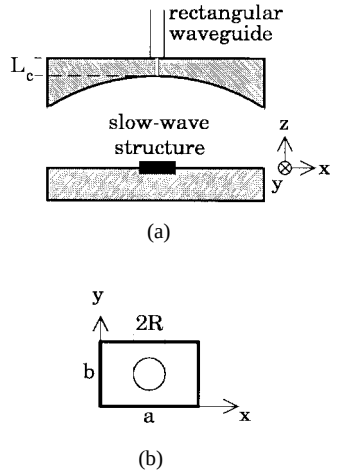

Fig. 2. (a) Orotron resonator. (b) Coupling aperture.

We apply Bethe's theory [11] for small coupling apertures, which has been modified by Collin [12], to the reflection-type orotron cavity shown in Fig. 2, in order to derive an equivalent circuit. The finite thickness of the coupling hole is taken into account by regarding the coupling hole as a circular waveguide with length L_c. The circuit parameters can be derived in closed form if the field in the cavity is given by a single mode. This assumption is confirmed by field-profile measurements in the cold orotron resonator. Finally, some experimental results are reported and compared with theory.

II. Modified Bethe Theory

In Bethe's theory of diffraction by small holes, the coupling between a waveguide and a resonator is described by electric and magnetic dipole moments at the position of the aperture following the principle of equivalence. These dipole moments

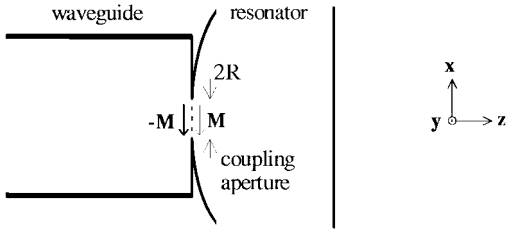

Fig. 3. Coupling by magnetic dipole moment.

are solely determined by the incident wave [11]. This approach has been modified by Collin introducing reaction terms, which describe the reduction of the dipole moments due to the influence of the resonator and of the reflected wave in the waveguide [12]. This theory has been applied to transmission-type open resonators by Mongia [13] without considering the finite thickness of the coupling aperture.

Due to the well-known field structure in a quasi-optical resonator, the coupling between the resonator and a waveguide is mainly given by tangential magnetic fields, since the normal component of the electric field is much smaller than the tangential magnetic field [14]. Considering the coupling hole as a circular waveguide, the coupling between this waveguide and the cavity can be described by the magnetic dipole moment $\boldsymbol{M}$ as follows:

$$\boldsymbol{M} = [\alpha] \cdot (\boldsymbol{H}_{\mathrm{wg},i} + \boldsymbol{H}_{\mathrm{wg},r} - \boldsymbol{H}_{\mathrm{cav},r}) \tag{1}$$

where $\boldsymbol{H}_{\mathrm{wg},i}$ signifies magnetic field of the incident wave, $\boldsymbol{H}_{\mathrm{wg},r}$ and $\boldsymbol{H}_{\mathrm{cav},r}$ are the reaction fields in the waveguide and the cavity, respectively, and $[\alpha]$ denotes dyadic magnetic polarizability of the aperture. The transition from the coupling hole to the resonator is closed by means of a conducting magnetic wall, as shown in Fig. 3.

Since the transversal magnetic field of the exciting mode in the rectangular waveguide TE_{10} only consists of an x-component, (1) can be reduced to the x-components of the dipole moment and the magnetic fields. The dyadic magnetic polarizability can be rewritten as a constant α_x. For a circular coupling hole of radius r_0, the magnetic polarizability is given by $\alpha_x = 4r_0^3/3$. Hence

$$M_x = \alpha_x \cdot (H_{\mathrm{wg},i_x} + H_{\mathrm{wg},r_x} - H_{\mathrm{cav},r_x}). \tag{2}$$

The magnetic field $H_{\mathrm{wg},i}$, due to the incident mode, can be evaluated from the fundamental TE_{11} mode in the circular waveguide. The transversal field can be derived using a normalized scalar potential [12]:

$$T_{h_{11}} = N_{h_{11}} \cdot J_1\left(\frac{p'_{11} \cdot r}{R}\right) \cdot \cos(\phi) \tag{3}$$

in cylindrical coordinates with the normalization factor

$$N_{h_{11}} = \sqrt{\frac{2}{(p'^2_{11} - 1) j k_0 Z_0 \Gamma_{11} \pi}} \cdot \frac{1}{J_1(p'_{11})}. \tag{4}$$

Here, k_0 is the wavenumber and Z_0 wave impedance in free space, Γ_{11} denotes the propagation constant of the TE_{11} mode, and R is the radius of the circular waveguide. J_1 is the Bessel function of the first kind and p'_{11} first zero of J'_1. The prime denotes differentiation with respect to the argument. The transversal magnetic field of the incident wave is then given by

$$H^+_{t_{11}} = \Gamma_{11} \cdot \nabla_t \cdot T_{h_{11}} \cdot e^{\Gamma_{11} z}. \tag{5}$$

The $+$ sign denotes a wave propagating in the positive z-direction. Due to the magnetic conducting wall at the end of the circular waveguide, the incident wave is completely reflected. Thus, the total magnetic field H_{wg,i_x} produced by the exciting wave at the center of the coupling hole can be expressed as

$$H_{\mathrm{wg},i_x} = (H^+_{x_{11}} - H^-_{x_{11}})|_{z=0} = 2 \cdot \Gamma_{11} \cdot N_{h_{11}} \cdot \frac{p'_{11}}{2R}. \tag{6}$$

The scattered magnetic field in the waveguide H_{wg,r_x} due to the presence of the magnetic dipole moment M_x is determined by [12]

$$H_{\mathrm{wg},r_x} = j\omega\mu_0 H^+_{x_{11}}(-M_x \boldsymbol{a}_x) H^-_{x_{11}} \boldsymbol{a}_x. \tag{7}$$

In (7), ω denotes the angular frequency and μ_0 is the magnetic permeability of vacuum. Substituting (5) in (7) results in

$$H_{\mathrm{wg},r_x} = \frac{M_x \cdot p'^2_{11} \cdot \Gamma_{h_{11}}}{2\pi R^2 (p'^2_{11} - 1) J_1^2(p'_{11})}. \tag{8}$$

The reaction term H_{cav,r_x}, which describes the reduction of M_x by the resonator field, can be expressed in terms of the normalized eigenfunctions of the cavity h_n following [12]:

$$H_{\mathrm{cav},r_x} = \frac{-k_0^2 \cdot M_x \cdot h_n^2}{k_{0r}^2 - k_0^2 \cdot \left(1 + \dfrac{(1-j)}{Q}\right)}. \tag{9}$$

In (9), k_{0r} signifies wavenumber at resonance, Q denotes the unloaded Q factor, and h_n the nth normalized eigenfunction of the resonator at the position of the coupling hole. The eigenfunctions are normalized with respect to the volume integral

$$\int_V \boldsymbol{h}_n \cdot \boldsymbol{h}_n \, dV = 1. \tag{10}$$

The x-component of the eigenfunction n is given by [14] to be

$$h_{n_x} = \frac{2}{w_0 \sqrt{2^{(m+n)} m! n! \pi D}} \cdot e^{(x^2+y^2)/w_0^2} \cdot H_m\left(\sqrt{2}\,\frac{x}{w_0}\right) \cdot H_n\left(\sqrt{2}\,\frac{y}{w_0}\right) \cdot \cos(k_0 z). \tag{11}$$

Here, w_0 signifies spot size of the fundamental $(m = n = 0)$ mode, m and n are the mode numbers in the x- and y-direction, respectively. D signifies distance between the mirrors, and H_m and H_n are the Hermite polynomials of order m and n, respectively. Since D is much smaller than the radius of curvature of the spherical mirror, the divergence of the phase front can be neglected. Inserting (6), (8), and (9) into (2) results in an expression for the reduced magnetic dipole moment:

$$M_x = \frac{2\alpha_m \Gamma_{h_{11}} \dfrac{p'_{11}}{2R} N_{h_{11}}}{1 + X - \alpha_m K} \tag{12}$$

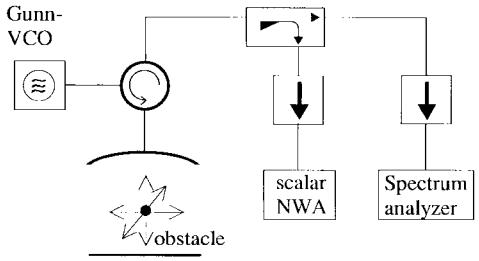

Fig. 4. Field-profile measurement setup.

where

$$X = \alpha_m \frac{p_{11}'^2 \Gamma_{h_{11}}}{2R^2\pi(p_{11}'^2 - 1)J_1^2(p_{11}')}$$

$$K = \frac{k_0^2 h_n^2}{k_{0r}^2 - k_0^2\left(1 + \dfrac{1-j}{Q}\right)}.$$

III. Resonator Fields

The theory given in Section II is valid only for single-mode operation, i.e., the field inside the cavity is well described by just one eigenfunction. Considering the well-known equation for the resonance frequency of a quasi-optical resonator [14]

$$f_{mnq} = \frac{c}{D}\left[q + \frac{1}{\pi}(m+n+1)\arctan\left(\frac{D}{z_0}\right)\right] \qquad (13)$$

this assumption holds for the fundamental $(m = n = 0)$ mode. For higher order modes, the modes $m + n = \text{constant}$ are degenerate. In (13), c is the velocity of light, q denotes the transversal index of the resonator mode, and z_0 is given by $z_0 = \sqrt{D(R_s - D)}$. R_s denotes radius of curvature of the spherical mirror.

The desired working mode in the orotron resonator is the TEM_{20q} mode [8]. This should be the only mode in the cavity close to resonance. In order to prove this assumption, the field pattern in the cavity has been measured moving a small obstacle through the cavity. The obstacle is built by a small metallic ball fixed on a thin thread. The obstacle perturbs the electric field inside the resonator, so that the stored electric energy is reduced. This causes a shift in the resonance frequency, which has been measured using the measurement setup shown in Fig. 4. The shift in resonance frequency is a function of the electric-field intensity at the position of the obstacle [15].

The field-profile measurements have been performed at 94 GHz. The distance between the mirrors D has been around 14.4 mm, corresponding to a transversal mode index $q = 9$. The first resonance at this transversal-mode index belongs to the fundamental $(m = n = 0)$ mode, and the second resonance is excited by the $(20q)$ and $(02q)$ modes. Since the coupling hole is located at the center of the upper mirror, modes with odd indexes in x- or y-direction are not excited.

In a first step, the field patterns of an ideal quasi-optical resonator, i.e., without slow-wave structure in the plane mirror, have been measured for these two resonances. Fig. 5 shows the field profile versus obstacle position with respect to the coordinate system in Fig. 2. The dashed lines give the field

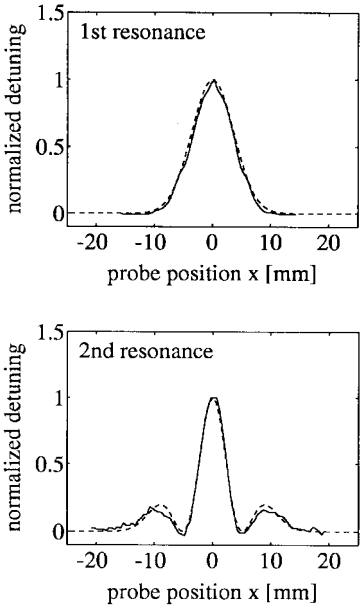

Fig. 5. Field patterns without grating (—: measurement, - - - : theory).

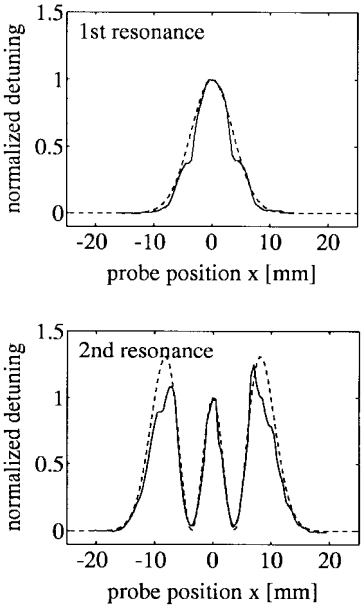

Fig. 6. Field patterns with grating (—: measurement, - - -: theory).

intensity calculated from (11) and normalized to the field intensity at the center of the resonator.

At the first resonance, the measured pattern agrees well with the theoretical fundamental profile. At the second resonance, the measured pattern is fitted well by a symmetrical superposition of the TEM_{20q} and TEM_{02q} modes. As expected, both modes are excited at this resonance. Hence, the theory of Section II cannot be applied for higher order modes in an empty quasi-optical resonator.

The same measurements have been performed for the orotron resonator, i.e., a slow-wave structure is mounted in the lower mirror. The slow-wave structure is designed for negligible perturbation of the TEM_{20q}-mode profile. Results have been plotted in Fig. 6.

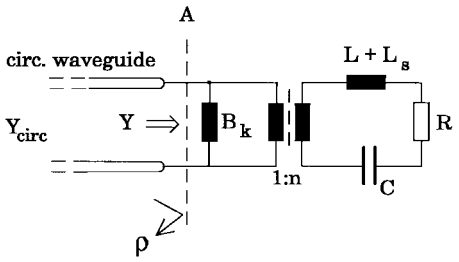

Fig. 7. Equivalent circuit of circular waveguide-to-resonator transition.

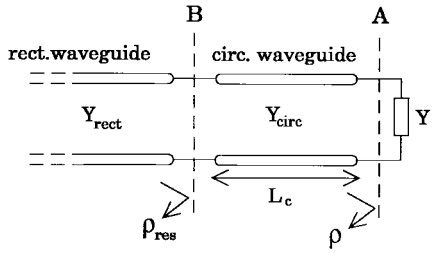

Fig. 8. Simple rectangular-to-circular waveguide transition.

At the first resonance, the Gaussian-shaped profile is strongly perturbed due to diffraction losses at the corners of the grating. In this experiment, the width of the grating has been 7.3 mm corresponding to the position of the perturbations in the field patterns. The dashed line denotes the unperturbed profile of the fundamental mode.

The insertion of the grating changes the field profile strongly at the second resonance. The dashed line gives the field intensity of the desired TEM_{20q} mode. It can be seen that the measured profile agrees very well with the theoretical one. Due to the additional losses by diffraction, the undesired TEM_{02q} mode is well suppressed. The perturbations in the side maxima are due to the used spherical mirror, since the spherical shape has been generated by small circular steps. Using a perfect spherical mirror leads to an improved profile, even in the side maxima.

The field-profile measurements verify the assumption of single-mode operation in the orotron resonator, even if operating at the higher order mode TEM_{20q}.

IV. Equivalent Circuit

The reflection coefficient of a short-circuited waveguide with a magnetic dipole moment at the center of the waveguide is given by [12] as

$$\rho = -1 + j\omega\mu_0 M_x \boldsymbol{a}_x H^+_{x_{11}}. \tag{14}$$

Substituting the reduced-dipole moment corresponding to (12) into (14) results in a simple expression for the reflection coefficient

$$\rho = -1 + \frac{2X}{1 + X - K\alpha_m}. \tag{15}$$

In order to determine an equivalent circuit, the corresponding input admittance Y_{res} can be calculated as

$$\frac{Y_{\mathrm{res}}}{Y_{\mathrm{circ}}} = \frac{1-\rho}{1+\rho} = \frac{1}{X} - \frac{k_0^2 h_n^2 \dfrac{\alpha_m}{X}}{k_{0r}^2 - k_0^2\left(1 + \dfrac{1-j}{Q}\right)}. \tag{16}$$

Y_{circ} means wave admittance of the fundamental TE_{11} mode in the circular waveguide. Fig. 7 shows the equivalent circuit of the open resonator, which is well suited to illustrate a formula of the same form as (16) [13]. The input admittance at the right-hand side of plane A is given by

$$\begin{aligned} Y &= -jB_k + \frac{n^2}{j\omega(L+L_s) + R - \dfrac{j}{\omega C}} \\ &= -jB_k + \frac{j\omega\omega_0^2 n^2 C}{\omega_0^2 - \omega^2\left(1 + \dfrac{1-j}{Q}\right)} \end{aligned} \tag{17}$$

where ω_0 represents the resonant angular frequency of the unloaded resonator, and is given by $\omega_0 = 1/\sqrt{LC}$. ω denotes the angular frequency close to resonance. A comparison between (16) and (17) results in closed-form expressions for the elements of the equivalent circuit:

$$\begin{aligned} B_k &= jY_{\mathrm{circ}} \frac{2R^2\pi(p_{11}'^2 - 1)J_1^2(p_{11}')}{\alpha_m \Gamma_{h_{11}} p_{11}'^2} \\ L &= \frac{1}{\omega_0^2 C} \\ L_s &= \frac{L}{Q} \\ R &= \frac{\omega_0 L}{Q} \\ n^2 &= B_k \alpha_m \frac{\omega^2 h_n^2}{\omega\omega_0^2 C} \\ C &= 1. \end{aligned} \tag{18}$$

The value for the capacitor is chosen to equal unity. In order to take the finite thickness of the coupling hole into account, the input admittance Y at plane A is transformed to plane B using transmission-line theory. Fig. 8 shows the complete transition.

The resulting reflection coefficient ρ_{res} must be calculated with respect to the wave admittance of the exciting TE_{10}-mode Y_{rect}:

$$\rho_{\mathrm{res}} = \frac{Y' - Y_{\mathrm{rect}}}{Y' + Y_{\mathrm{rect}}} \tag{19}$$

where

$$Y' = Y_{\mathrm{circ}} \frac{Y + Y_{\mathrm{circ}} \tanh(\Gamma_{11} L_c)}{Y_{\mathrm{circ}} + Y \tanh(\Gamma_{11} L_c)}. \tag{20}$$

With (19), the resonant behavior of the hole setup corresponding to Fig. 2 is described by the geometrical parameters of the resonator and of the coupling hole, and by the unloaded Q factor of the open resonator. In order to use the equivalent circuit for designing the coupling hole with a desired coupling, either Q must be measured independently [13] or it must be calculated.

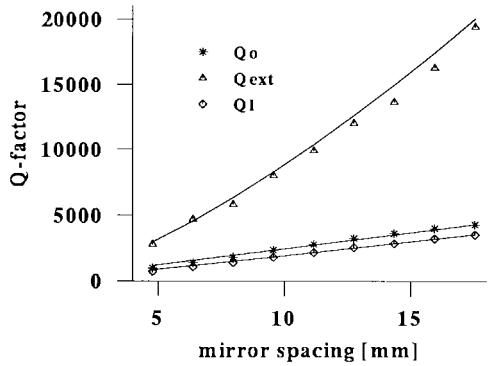

Fig. 9. Q factors for various mirror spacings (—: theory, $\diamond$, Δ, $\star$: measurement).

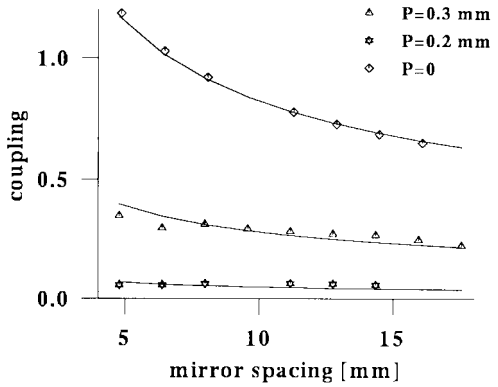

Fig. 10. Coupling for various mirror spacings Parameter: grating pitch p ($p = 0$: no grating, —: theory, $\diamond$, Δ, $\star$: measurement).

In this theory, the ohmic losses in the open cavity are calculated using skin-effect formulas [16] for a given conductivity of the used material. Diffraction losses are neglected, since the distance between the mirrors, D, is kept small. The additional ohmic losses due to the slow-wave structure are calculated using a correction term [8].

V. Measurements

The measurements have been performed with the vector network-analyzer HP8510C extension to W-band at 94 GHz. The analyzer has been calibrated with respect to plane B in Fig. 8. The mirror spacing has been controlled with an accuracy of 1.25 μm by means of a stepped motor. Both mirrors are made from pure oxid-free high-conductivity (OFHC) copper. The coupling hole shows a diameter $R = 0.65$ mm. The length of the coupling hole has been measured mechanically to be $L_c = 0.25$ mm. The output waveguide is realized as standard W-band rectangular waveguide ($a = 2.54$ mm, $b = 1.27$ mm). For measurements with a slow-wave structure, the plane mirror is completely replaced by another copper-made mirror containing the grating.

The computation of the coupling has been done by evaluating the frequency-dependent reflection coefficient $\rho_{\rm res}$ at a detuned–short position [17]. The coupling of a resonator is defined by

$$\kappa = \frac{Q}{Q_{\rm ext}} \tag{21}$$

where $Q_{\rm ext}$ means external Q.

The validity of the theory has been tested by measuring the resonant characteristics of an open resonator operating at the fundamental mode. The results of these measurements have been depicted in Fig. 9. The unloaded Q factor Q_0, as well as the loaded Q factor $Q_{\rm load}$, and the external Q factor $Q_{\rm ext}$, are plotted versus mirror spacing. Each marker denotes the measurement result for one transversal-mode index q.

The simulated and measured data correspond very well. This agreement has been obtained by assuming an electrical conductivity of the mirrors, which is less than the theoretical value by a factor of three. This fit has only been done once for the first data point in Fig. 9. This modified conductivity has been used in all of the following simulations presented in this paper.

For small mirror spacings, $Q_{\rm load}$ increases linearly with D, while the external Q factor $Q_{\rm ext}$ increases with $D^{1.5}$. These dependencies have been derived in [13]. Hence, the coupling κ corresponding to (21) can be described as $\kappa \propto 1/\sqrt{D}$. This behavior is shown in Fig. 10. The coupling κ is plotted versus mirror-spacing D. The plots include data of different arrangements. The rectangular markers denote the results of an open resonator without slow-wave structure operating with the fundamental TEM_{00q} mode. The triangles as well as the stars give the data of the orotron resonator with different slow-wave structures operating with the TEM_{20q} mode. The grating pitch varies from 0.3 mm (Δ) to 0.2 mm ($\star$). The grating with the smaller pitch must have a larger surface. Hence, the ohmic losses become larger, decreasing the unloaded Q factor.

The coupling κ decreases with mirror spacing as expected. Furthermore, the insertion of a slow-wave structure in the lower mirror decreases the coupling due to additional losses. The coupling can be predicted quiet well if the surface conductivity of the used material is known.

Fig. 11 shows the measured and simulated frequency-dependent reflection coefficient $\rho_{\rm res}$ plotted in the Smith chart for the orotron resonator operating with the TEM_{209} mode at 94 GHz. The circles denote the measured data. In Fig. 11(a), the data are plotted referred to the measurement plane B corresponding to Fig. 8. In Fig. 11(b), both curves are transformed to the detuned short position [17]. In Fig. 11(b), the data agree very well, even in the complex plane, so that both coupling κ and resonant behavior of the orotron cavity are well described. The most conspicuous difference between theory and measurement stems from the reactance far away from resonance, as shown in Fig. 11(a). In this example, the measured reactance is much smaller than the calculated reactance. This deviation is probably due to the very simple model for the rectangular-to-circular waveguide transition. Using a more sophisticated model for this transition should also result in better agreement for the coupling reactance.

According to [18], the coupling should be corrected by a factor for large coupling holes, i.e., $R \leq \lambda$. Although the coupling-hole radius in this experiment was rather large, the agreement between measurement and theory is quite good. This is due to taking the coupling-hole thickness into account. If the coupling hole is rather thick in comparison to the propa-

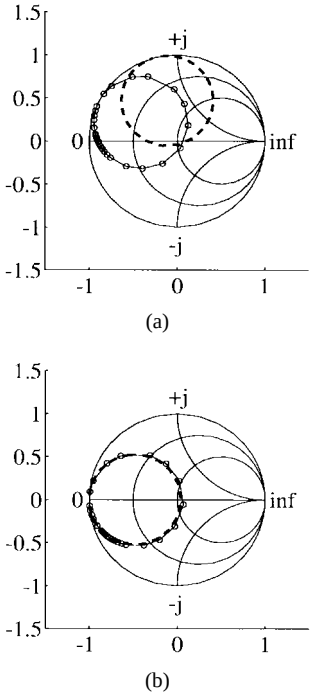

Fig. 11. (a) Complex reflection coefficient at plane of measurement and (b) detuned short position (- - -: theory, ∘: measurement).

gation coefficient in the coupling-hole region, the reduction of the coupling by the finite wall thickness is the most important effect. For very thin coupling holes, other effects like the influence of the waveguide walls [5] or large coupling-hole diameters [18] must be taken into account.

VI. Conclusions

Bethe's coupling theory for small holes has been modified for an application to the millimeter-wave orotron resonator. The finite thickness of the coupling hole has been taken into account. The field profile in an open resonator has been measured with and without slow-wave structures inside the resonator. The coupling has been described using an equivalent circuit, whose parameters are given in closed form. The agreement between measurement and theory was good for rather thick coupling holes. At millimeter waves, the thickness of the coupling hole is the most important parameter. The theory is suitable for the design of coupling holes in the millimeter-wave region.

Acknowledgment

The authors are indebted to the Institut für Hochfrequenztechnik at the Technische Universität Braunschweig, Germany, for using the W-band extended vector network-analyzer HP8510C.

References

[1] H. Kogelnik and T. Li, "Laser beams and resonators," *Proc. IEEE*, vol. 54, pp. 1312–1329, Oct. 1966.
[2] G. D. Boyd and J. P. Gordon, "Confocal multimode resonator for millimeter through optical wavelength masers," *Bell Syst. Tech. J.*, vol. XL, no. 2, pp. 489–508, Mar. 1961.
[3] P. K. Yu and A. L. Cullen, "Measurement of permittivity by means of an open resonator—Part I: Theoretical," in *Proc. R. Soc.*, London, U.K., 1982, pp. 49–71.
[4] M. N. Afsar, "Dielectric measurements of millimeter-wave materials," *IEEE Trans. Microwave Theory Tech.*, vol. MTT-32, pp. 1598–1609, Dec. 1984.
[5] V. N. Rodionova and G. Y. Slepyan, "The coupling of an open resonator with a rectangular waveguide,"*Radioteknika i Elektronika*, no. 7, pp. 1358–1365, 1989.
[6] O. M. Bucci and G. Di, "Open resonators powered by a rectangular waveguide," *Proc. Inst. Elect. Eng.*, vol. 139, pt. H, no. 4, pp. 323–329, 1989.
[7] F. S. Rusin and G. D. Bogomolov, "Generation of electromagnetic oscillations in an open resonator," *JETP Lett.*, no. 4, p. 160, 1966.
[8] D. E. Wortman and R. P. Leavitt, "The orotron," *Infrared and Millimeter Waves*, vol. 7. New York: Academic, 1983, pp. 322–375.
[9] G. Faby, S. Lütgert, and K. Schünemann, "Simulation of orotron performance for nonhomogeneous electron beam," in *IEEE Int. Conf. Infrared Millimeter Waves Conf. Dig.*, Orlando, FL, Dec. 1995, pp. 76–77.
[10] G. D. Bogomolov and F. S. Rusin, "An open cavity with variable quasioptical coupling," *Radio Eng. Electron. Phys.*, no. 16, pp. 727–729, 1970.
[11] H. A. Bethe, "Theory of diffraction by small holes," *Phys. Rev.*, vol. 66, no. 7/8, pp. 163–182, 1944.
[12] R. E. Collin, *Field Theory of Guided Waves.* Piscataway, NJ: IEEE Press, 1991.
[13] R. K. Mongia and R. K. Arora, "Equivalent circuit parameters of an aperture coupled open resonator cavity," *IEEE Trans. Microwave Theory Tech.*, vol. 41, pp. 1245–1250, Aug. 1993.
[14] S. Lütgert, "Konistente Analyze des Orotrons im Zeit- and Frequenzbereich," Ph.D. dissertation, Dept. High-Frequency Tech., Univ. Hamburg–Harburg, Germany, 1993.
[15] R. F. Harrington, *Time-Harmonic Electromagnetic Fields.* New York: McGraw-Hill, 1961, pp. 317–380.
[16] J. D. Jackson, *Classical Electrodynamics*. New York: Wiley, 1960, p. 130.
[17] M. Sucher and J. Fox, *Microwave Measurements*, vol. II. New York: Wiley, 1963.
[18] S. B. Cohn, "Microwave coupling by large apertures," *Proc. IRE*, vol. 40, pp. 696–699, June 1952.

G. Faby was born on March 12, 1963, in Stade, Germany. He received the Dipl.-Ing. degree in electrical engineering from the Technische Universität Braunschweig, Germany, in 1990, and is currently working toward the Ph.D. degree.

Since 1990, he has been a Research Assistant with the Arbeitsbereich für Hochfrequenztechnik, Technische Universit Ḧamburg–Harburg, Hamburg, Germany. His fields of interest include solid-state microwave power amplifiers, open resonators, power generation at millimeter-waves, and laser-diode modeling.

K. Schünemann (M'76–SM'86–F'95) was born in Braunschweig, Germany, in 1939. He received the Dipl.-Ing. degree in electrical engineering and the Doktor-Ing. degree from the Technische Universität Braunschweig, Germany, in 1965 and 1969, respectively.

Since 1983, he has been a Professor of electrical engineering and Director of the Arbeitsbereich Hochfrequenztechnik at the Technische Universit Ḧamburg–Harburg, Hamburg, Germany. He has worked on nonlinear microwave circuits, diode modeling, solid-state oscillators, PCM communication systems, and integrated-circuit technologies such as finline and waveguide-below-cutoff. His current research interests are concerned with transport phenomena in submicron devices, CAD of planar millimeter-wave circuits, optoelectronics, and high-power millimeter-wave tubes.